

AperTO - Archivio Istituzionale Open Access dell'Università di Torino

**Amino groups modified SBA-15 for dispersive-solid phase extraction in the analysis of micropollutants by QuEChERS approach**

**This is the author's manuscript**

*Original Citation:*

*Availability:*

This version is available <http://hdl.handle.net/2318/1788783> since 2021-05-14T08:13:28Z

*Published version:*

DOI:10.1016/j.chroma.2021.462107

*Terms of use:*

Open Access

Anyone can freely access the full text of works made available as "Open Access". Works made available under a Creative Commons license can be used according to the terms and conditions of said license. Use of all other works requires consent of the right holder (author or publisher) if not exempted from copyright protection by the applicable law.

(Article begins on next page)

1 **Amino groups modified SBA-15 for dispersive-solid phase extraction in the analysis of**  
2 **micropollutants by QuEchERS approach**

3

4

5 Michele Castiglioni<sup>a</sup>, Barbara Onida<sup>b\*</sup>, Luca Rivoira<sup>a</sup>, Massimo Del Bubba<sup>c</sup>, Silvia Ronchetti<sup>b</sup>,  
6 Maria Concetta Bruzzone<sup>a\*</sup>

7

8 <sup>a</sup> Department of Chemistry, University of Turin, Via P. Giuria 7, 10125 Turin, Italy

9 <sup>b</sup> Department of Applied Science and Technology, DISAT, Polytechnic of Turin, Corso Duca degli  
10 Abruzzi 24, 10129 Turin, Italy

11 <sup>c</sup> Department of Chemistry “Ugo Schiff”, University of Florence, Via della Lastruccia 3, 50019  
12 Sesto Fiorentino, Florence, Italy

13

14 **\*Corresponding Authors**

15 Prof. Maria Concetta Bruzzone

16 ORCID ID 0000-0002-9144-9254

17 Department of Chemistry

18 University of Turin

19 Via P. Giuria 7, 10125 Turin, Italy

20

21 **And**

22

23 Prof. Barbara Onida

24 ORCID ID 0000-0002-1928-3579

25 Department of Applied Science and Technology

26 DISAT, Polytechnic of Turin

27 Corso Duca degli Abruzzi 24, 10129 Turin, Italy

28

## Abstract

In the analysis of contaminants in food products, sample preparation is performed by proper adsorbents, whose choice is crucial to eliminate matrix interference. In this work we modified SBA-15 adsorbents by functionalization with (3-aminopropyl)-triethoxysilane (SBA-15-APTES) and N-[3-(trimethoxysilyl)propyl]aniline (SBA-15-AN) aiming to use them for the first time in the clean-up step of a QuEChERS (quick, easy, cheap, effective, rugged and safe) extraction of micropollutants from strawberry, a sugar rich fruit. After physico-chemical characterization by nitrogen adsorption, infrared spectroscopy and thermogravimetric analysis, the adsorption capabilities of SBA-15 sorbents and possible interaction mechanisms were studied at different pH (2.1-8.5) for glucose, sucrose and fructose at concentrations characteristic of those found in strawberries. The performance of the two SBA-15 sorbents was compared with that of commercial PSA (primary secondary amine), usually proposed in QuEChERS protocols. Both SBA-15 materials exhibit up to 30% higher adsorption than PSA, suggesting their possible QuEChERS application. Synthesized SBA-15 adsorbents were hence used as innovative dispersive sorbents in the QuEChERS extractions of 13 PAHs and 14 PCBs from strawberry. For PCBs, SBA-15-AN provides better matrix removal than PSA and comparable extraction recoveries around 90%. For PAHs, the use of SBA-15-AN has the advantage of lower relative standard deviation (7%) than PSA (19%).

**Keywords:** QuEChERS food analysis, *d*-SPE, sugar removal, SBA-15 mesoporous silica, functionalization

## 1. Introduction

Fruits and their transformation products (e.g. beverages and jams) may be altered by organic micropollutants due to many contamination sources, such as soil and irrigation water [1, 2], as well as packaging materials [3] and pesticide application [4].

Current regulation regarding the presence of organic micropollutants in fruits and vegetables includes polycyclic aromatic hydrocarbons (PAHs), polychlorinated dibenzo(p)dioxins (PCDDs), polychlorinated dibenzo(p)furans (PCDFs), and polychlorinated biphenyls (PCBs) with dioxin-like properties, referred to as dioxine-like PCBs (DL-PCBs) [5].

Most of the above-mentioned compounds in fruits and derived products are analysed by using the QuEChERS approach followed by gas chromatographic-mass spectrometric analysis (GC-MS) [2, 6]. QuEChERS extraction is based on the partition of target analytes between water and acetonitrile.

62 Sugars present as natural components or as additives are well-known interferents in the  
63 QuEChERS approach since they are co-extracted in acetonitrile and must be removed prior to the  
64 analysis of the extracted samples by chromatographic methods.

65 This task is usually accomplished using solid-phase extraction (SPE) cleanup, even through  
66 on-line approaches [7], or by a dispersive solid phase extraction (*d*-SPE) clean-up step, with a primary  
67 secondary amine (PSA) sorbent [8, 9]. Several manufacturers make commercially available  
68 proprietary PSA sorbents which are based on silica chemically modified with ethylenediamine-N-  
69 propyl group, as bulk packing, or within ready-to-use kits for QuEChERS analysis. PSA is usually  
70 claimed to be a sorbent more retentive than aminopropyl phases due to presence of the secondary  
71 amine [10], even if dedicated studies on the adsorption mechanisms are not yet available.

72 Ordered mesoporous silicas and organosilicas have been largely investigated as adsorbents  
73 [11-14] due to their high specific surface area and uniform porosity, together with the possibility of  
74 tailoring their surface chemical properties through synthesis conditions and post-synthesis  
75 modification. In particular, in the context of analytical chemistry, ordered mesoporous organosilicas  
76 have been tested as adsorbents for food samples cleanup [15].

77 Mesoporous silica functionalized with amino groups was previously investigated for  
78 adsorption and removal of anionic pollutants in wastewater [16, 17].

79 The aim of this work is to synthesize and study the performance of organically modified  
80 ordered mesoporous silicas to be innovatively included as *d*-SPE sorbents in a QuEChERS protocol  
81 for the removal of co-extracted sugars for the analysis of contamination of strawberries by 13 PAHs  
82 and 14 PCBs, including dioxine-like congeners. PCBs and PAHs are often found in fruit [18, 19] and  
83 are therefore a major concern for health protection.

84 Ordered mesoporous silica of SBA-15 family was functionalized with the primary amine (3-  
85 aminopropyl)-triethoxysilane (APTES) and, in another case, with the secondary amine N-[3-  
86 (Trimethoxysilyl)propyl]aniline, in order to mimic the commercial PSA. After the determination of  
87 the main physico-chemical characteristics, the adsorption of glucose, fructose and sucrose (sugars  
88 naturally contained in fruit) was studied. The performances of the two organically modified SBA-15  
89 silica as QuEChERS *d*-SPE sorbents were investigated determining the signal to noise ratio and the  
90 extraction recoveries for target compounds, in comparison with those obtained by commercial PSA.

91 To the best of our knowledge no reports are currently available on the use of ordered  
92 mesoporous organosilicas in the QuEChERS technique.

93

## 94 **2. Materials and Methods**

### 95 *2.1 Reagents*

96 All reagents used were of analytical grade. Ordered mesoporous silica of the SBA-15 type  
97 was purchased from ACS Material Advanced Chemical Supplier (Pasadena, CA, USA). (3-  
98 aminopropyl) triethoxysilane (APTES, 99%), N-[3-(Trimethoxysilyl)propyl]aniline, toluene  
99 (99.8%), acetonitrile (>99.9%) were purchased from Sigma Aldrich (Steinheim, DE). Primary  
100 Secondary Amine (PSA, Figure 1A) was purchased from Agilent Technologies (Santa Clara, CA,  
101 USA). D(+) glucose was purchased from Merck (Darmstadt, DE), D(-) fructose and sucrose were  
102 purchased from J.T. Baker (Phillipsburg, NJ, USA).

103 The PAHs studied were the 13 PAH compounds listed by EPA 525.1 procedure and were  
104 purchased from Sigma Aldrich-Merck (Darmstadt, Germany): acenaphthylene (AcPY), fluorene (Flu),  
105 phenanthrene (Phe), anthracene (Ant), pyrene (Pyr), benzo[a]anthracene (BaA), chrysene (Chr),  
106 benzo[b]fluoranthene (BbFl), benzo[k]fluoranthene (BkFl), benzo[a]pyrene (BaP), indeno[1,2,3-  
107 cd]pyrene (Ind), dibenzo[a,h]anthracene (DBA), benzo[ghi]perylene (BP). PCBs were purchased  
108 from LGC Standards (Milan, Italy). They were non-dioxine like PCBs: 3,3'-dichlorobiphenyl (PCB  
109 11), 4,4'-dichlorobiphenyl (PCB 15), 2,4,4'-trichlorobiphenyl (PCB 28), 2,2',5,5'-  
110 tetrachlorobiphenyl (PCB 52), 2,2',4,5,5'-pentachlorobiphenyl (PCB 101), 2,2',3,4,4',5'-  
111 hexachlorobiphenyl (PCB 138), 2,2',4,4',5,5'-hexachlorobiphenyl (PCB 153), 3,3',4,4',5,5'-  
112 hexachlorobiphenyl (PCB 169), 2,2',3,4,4',5,5'-heptachlorobiphenyl (PCB 180), 2,3,3',4,4',5,5'-  
113 heptachlorobiphenyl (PCB 189); and dioxine like PCBs: 3,4,4',5-tetrachlorobiphenyl (PCB 81),  
114 2,3',4,4',5-pentachlorobiphenyl (PCB 118), 2',3,4,4',5-pentachlorobiphenyl (PCB 123),  
115 2,3',4,4',5,5'-hexachlorobiphenyl (PCB 167).

116 Hydrochloric acid (35% w/w,  $d = 1.187 \text{ g/mL}$ ) and NaOH (>98%) were from Carlo Erba  
117 (Milano, IT). NaCl,  $\text{MgSO}_4 \cdot 7\text{H}_2\text{O}$  and  $\text{H}_2\text{SO}_4$  (95–97%,  $d = 1.84 \text{ g/mL}$ ) were from Sigma-Aldrich.  
118 High-purity water (18.2 M  $\Omega \cdot \text{cm}$  resistivity at 25°C), produced by an Elix-Milli Q Academic system  
119 from Millipore (Vimodrone, MI, Italy) was used for standard and eluent preparation.

120

## 121 2.2 Preparation of sorbents

122 The synthesis procedures of the two sorbents were based on previous work concerning on the  
123 functionalization of SBA-15 silica [16, 17]. In a flask, 1 g of SBA-15, previously washed with about  
124 50 mL of deionized water, was stirred with 200 mL of toluene for 30 min, at room temperature.  
125 Afterwards, 2 mL of functionalizing reagent ((3-aminopropyl)-triethoxysilane-APTES or N-[3-  
126 (trimethoxysilyl)propyl]aniline, Fig. 1B and 1C) was added dropwise. The flask was then connected  
127 to a water-refrigerated system and the solution heated to 110 °C. The solution was kept under stirring  
128 for 24 hours. Afterwards, the powder was filtered and dried.

129 Hereafter the sample functionalized with APTES is denoted SBA-15-APTES and the sample  
130 functionalized with N-[3-(trimethoxysilyl)propyl]aniline is denoted SBA-15-AN.

131

### 132 *2.3 Physico-chemical characterization*

133 Nitrogen adsorption isotherms were measured using a Quantachrome AUTOSORB-1  
134 (Boynton Beach, FL, USA) instrument. Prior to nitrogen adsorption, samples were outgassed at 393  
135 K for 6 h. The BET specific surface areas (SSA) were calculated in the relative pressure range from  
136 0.04 to 0.1 and the pore size distribution were determined through the NLDFT (Non Localized  
137 Density Functional Theory) method, using the equilibrium model for cylindrical pores.

138 For FTIR measurements, powders were pressed in self-supporting wafers and spectra were  
139 recorded at room temperature with a Bruker Tensor 27 (Bruker, Billerica, MA, USA) spectrometer  
140 operating at  $2\text{ cm}^{-1}$  resolution, after outgassing the sample at room temperature (residual pressure of  
141 0.1 Pa).

142 TG analyses were carried out between 298 K and 1073 K in air (flow rate 100 mL/min with a  
143 heating rate of 10 K/min) using a SETARAM 92 (Caluire, France) instrument.

144 Density functional theory (DFT) simulations were calculated by means of Gaussian 09W and  
145 Gaussian View (Gaussian Inc, Wallington, US).

146

### 147 *2.4 Chromatographic analysis*

148 The evaluation of sugar content was performed by ion-chromatography using an ICS-3000  
149 gradient pump, Thermo Fisher Scientific, Waltham, MA, USA, coupled to pulsed amperometric  
150 detection. An AD40 Electrochemical Detector, Thermo Fisher Scientific, equipped with Ag/AgCl  
151 reference electrode and a gold working electrode was used. The detection potential was set at 0.1 V  
152 and maintained for 400 ms: the first 200 ms represents the delay time and the second 200 ms  
153 represents the determination time. The potential was then instantaneously set at -2 V and maintained  
154 for 10 ms and raised at 0.6 V and maintained for 10 ms to restore the gold oxide necessary to maintain  
155 an active working electrode surface. The potential was finally set at -0.1V and maintained for 60 ms,  
156 to reduce the small amount of gold oxide previously formed. The waveform requires a total of 500  
157 ms.

158 The sample (10  $\mu\text{L}$ ) was injected through a six-ways Rheodyne injection valve. The column  
159 used was a CarboPacPA10, 250x4 mm (100  $\mu\text{eq}/\text{column}$ ), Thermo Fisher Scientific which has a  
160 microporous substrate with particle size of 10  $\mu\text{m}$ , 55% cross-linking functionalized with a  
161 difunctional quaternary ion latex (5% cross-linking).

162 After optimization, the eluent concentration was kept at 55 mM KOH (data available upon  
163 request). At these conditions, limits of detection (LODs) for glucose, fructose and sucrose, calculated  
164 as  $s_m = s_m + 3s_b$ , with  $s_m$ =average signal of blank,  $s_b$ = standard deviation of blank on ten measurements,  
165 were respectively 69, 56 and 11  $\mu\text{g/L}$ . Pump, detector settings, and data collection were managed by  
166 the Chromeleon v.6.80 software (Thermo Fisher Scientific).

167 For PAHs and PCBs analysis, a gas chromatographic-mass spectrometric (GC-MS) method  
168 was used, according to previous studies by our research group [2, 20], employing an Agilent (Santa  
169 Clara, CA,USA) 6980 series gas chromatograph coupled with an Agilent 5973 Network mass  
170 spectrometer detector.

171 The GC column was a (5%-Phenyl)-methylpolysiloxane column (HP 5ms, 30 m x 0.25 mm x  
172 25  $\mu\text{m}$ , Agilent), with He as gas carrier (1 mL/min). MS detection was performed in Single Ion  
173 Monitoring (SIM) mode, selecting for each analyte its proper m/z ratio (m/z ratio available upon  
174 request). 2  $\mu\text{L}$  of each sample were injected using the Pulsed Splitless mode (pressure at 40 psi for  
175 2.5 min). The oven ramp was: 90°C, hold for 2 min; ramp to 176 °C, 12 °C/min rate; ramp to 196°C,  
176 5 °C/min rate, hold for 3 mins; ramp to 224°C, 12 °C/min rate; ramp to 244 °C, 5°C/min rate, hold  
177 for 3 min; ramp to 270 °C, 7°C/min rate, hold for 3 min; ramp to 300 °C, 5°C/min, hold for 10 min  
178 to completely clean and restore the GC column. The total run time for the complete separation of  
179 PAHs and PCBs is 52 min.

180 LODs, calculated as previously described for ion chromatography, were in the range from  
181 0.06  $\mu\text{g/L}$  (BaA) to 2.10  $\mu\text{g/L}$  (DBA), while from 0.49  $\mu\text{g/L}$  (PCB153) to 5.40  $\mu\text{g/L}$  (PCB169).  
182 Detailed analytical features of the GC-MS method are presented in Table S1 (for PAHs) and S2 (for  
183 PCBs) of the Supplementary Information section.

184 GC-MS data were handled with OpenChrome software (Lablicate, Germany).

185

### 186 *2.5 Adsorption tests*

187 Tests to evaluate the effect of pH were performed on 0.25 g of sorbent. The sorbent was put  
188 in contact with 4 g solution containing 350 mg/g glucose, 350 mg/g fructose and 170 mg/g sucrose.  
189 These concentrations were chosen in order to match those contained in strawberry according to  
190 Kasperbauer [21]. Solutions were stirred at 1100 xg for 10 min. Experiments were performed at pH  
191 2.1, 5.0 and 8.5.

192

### 193 *2.6 Strawberry fruits*

194 Commercial strawberry samples grown in Italy were used. *Fragaria x ananassa*, *Camarosa*  
195 cultivar was chosen as model plant, since it accounts for about 60% of the strawberry world's  
196 production and it adapts greatly to wide climate and growth conditions.

197

### 198 2.7 Extraction of PAHs and PCBs from strawberries by QuEChERS

199 Among organic micropollutants, PCBs and PAHs, present in the environment as a result of  
200 natural and anthropogenic processes, represent both point source and diffuse emissions [22].

201 PAHs and PCBs were extracted using a QuEChERS approach [8, 23]. Briefly, 5 g of  
202 homogenized strawberries were put in a vial containing 10 mL acetonitrile:H<sub>2</sub>O pH 2.1 (70:30), 8.2  
203 g MgSO<sub>4</sub> and 1 g NaCl. The tube was vigorously shaken and centrifuged at 1100 xg for 10 min. After  
204 extraction, a 4 mL aliquot of the supernatant was then transferred in a new vial containing 0.25 g of  
205 sorbent (PSA or SBA-15-APTES or SBA-15-AN) and 1.0 g MgSO<sub>4</sub> for the clean-up step. The tube  
206 was shaken and centrifuged (7870 xg, 10 min) and the supernatant was directly analysed by GC-MS.  
207 For each sorbent, the recovery was calculated spiking the fruit samples prior- (i) and post- (ii)  
208 extraction as follows:

- 209 • Pre-extraction spike: a cumulative batch of 50 g of homogenised strawberries was spiked with  
210 6666 µL of a solution containing PAHs and PCBs at 300 µg/L each, to achieve a final  
211 concentration of 0.04 mg/kg. According to the extraction procedure above detailed, a  
212 theoretical final concentration of 20 µg/L is expected for each PAH and PCBs. The procedure  
213 was repeated in triplicate.
- 214 • Post-extraction spike: after the extraction and clean-up procedure, 187 µL of the extract is  
215 spiked with 13 µL of the solution containing PAHs and PCBs at 300 µg/L, so to obtain a final  
216 concentration of 20 µg/L for each PAH and PCBs. The procedure was repeated in triplicate.

217

218 For each analyte, extraction recovery percentage (ER%) was calculated from the peak areas  
219 obtained after the pre-extraction spike ( $A_{\text{pre-extraction}}$ ) and post-extraction ( $A_{\text{post-extraction}}$ ) according to  
220 the equation:

$$221 \text{ER}\% = 100 * A_{\text{pre-extraction}} / A_{\text{post-extraction}}$$

222

223 For each analyte and experimental conditions, signal-to-noise ratio (S/N) was derived from  
224 the software OpenChrome and was calculated from the height of the analyte chromatographic peak  
225 ( $H_{\text{peak}}$ ) and that of the noise ( $h_{\text{noise}}$ ), according to the 2015 United States Pharmacopeia definition [24]:

$$226 \text{S/N} = 2H_{\text{peak}}/h_{\text{noise}}$$

227



### 3. Results and discussion

#### 3.1 Physico-chemical characterization

Table 1 reports textural features of SBA-15 as such and of functionalized SBA-15. For both SBA-15-APTES and SBA-15-AN, lower values of SSA, pore volume and pore diameter are observed with respect to the pristine SBA-15. These results reveal that grafting of organic moieties on the internal surface of silica mesopores occurred during functionalization.

N<sub>2</sub> adsorption measurement was carried out also on PSA since no data for the commercial product were available. It is worth noting that the same features of PSA are in between those of SBA-15 and organically modified SBA-15, so that, as a whole, we can consider PSA, SBA-15-APTES and SBA-15-AN comparable systems for the proposed QuEChERS application.

Fig. 2 shows FT-IR spectra of SBA-15, SBA-15-APTES and SBA-15-AN after outgassing at room temperature.

The spectrum of SBA-15 (curve 1) reveals the typical features of an amorphous silica, i. e. the narrow band at 3743 cm<sup>-1</sup>, due to the stretching mode of isolated silanols, and the broad band centred at 3530 cm<sup>-1</sup>, due to H-bonded silanols.

In the spectrum of SBA-15-APTES (curve 2), bands due to the organic moieties are clearly observed, that are: i) two bands at 3355 cm<sup>-1</sup> and 3295 cm<sup>-1</sup> attributed to the stretching modes of -NH<sub>2</sub> groups; ii) two bands at 2930 cm<sup>-1</sup> and 2875 cm<sup>-1</sup> due to the stretching modes of aliphatic -CH<sub>2</sub>- groups; iii) a band at about 1595 cm<sup>-1</sup> due to the bending mode of -NH<sub>2</sub> groups. As usually observed for amorphous silica modified with APTES, a broad and ill-defined absorption is observed at about 3000 cm<sup>-1</sup>, on which the previous mentioned bands are superimposed. This absorption is due to the residual silanols engaged in H-bonding with surface -NH<sub>2</sub> groups [25]. Indeed, in the spectrum, the stretching mode of isolated silanols is not present.

In the case of SBA-15-AN (curve 3), as for SBA-15-APTES, the bands due to the organic groups are visible in the spectrum, i.e. i) the band at 3330 cm<sup>-1</sup> due to the stretching mode of -NH-species; ii) bands above and below 3000 cm<sup>-1</sup> due to, respectively, aromatic -CH and aliphatic -CH<sub>2</sub>- stretching modes; iii) bands below 1700 cm<sup>-1</sup> due to ring modes of the aromatic moieties. Moreover, a broad absorption is observed at about 3600 cm<sup>-1</sup> which is tentatively ascribed to the residual silanols engaged in H-bonding with aromatic rings [26].

In summary, the set of IR data reveal that amine species in modified SBA-15 are located and exposed on the silica surface, in agreement with textural features (Table 1) discussed above.

From TG curves (not reported), the amount of amino groups was estimated and it is 4.41 mmol/g for SBA-15-APTES and 2.23 mmol/g for SBA-15-AN.

262 According to data found for commercially available PSA in the market, capacity for PSA  
263 ranges from 0.65 to 1.22 mmol/g [27, 28]. The above-mentioned capacity data suggest, per se, a  
264 competitive performance of functionalized SBA-15 in respect to PSA, and supports the study herein  
265 proposed.

266

### 267 *3.2 Adsorption measurements*

268 The following experiments were performed in order to optimize the pH conditions to be used  
269 in QuEChERS application. Furthermore, the results may be useful in formulating possible  
270 interactions acting between adsorbents and sugars during retention.

271 Results are represented in Fig. 3A, 3B, 3C. According to the acidic dissociation constants of  
272 the sugars considered ( $pK_a=12.2$  for glucose, 12.0 for fructose and 12.6 for sucrose), the concentration  
273 of dissociated sugars may be considered negligible at pH values studied (2.1, 5.0 and 8.5).

274 Organically modified mesoporous silicas show better removal performance than commercial  
275 PSA for all the pH values. It is worth noting that textural properties such as SSA and pore volume of  
276 SBA-15-APTES and SBA-15-AN are comparable to those of PSA (see Table 1), therefore the better  
277 adsorption performance of organically modified mesoporous silica has to be ascribed to the functional  
278 groups acting as adsorption sites, the amount of which is larger in SBA-15-APTES and SBA-15-AN  
279 than in PSA. Nevertheless, a role of different surface chemical properties of the two silica supports,  
280 cannot be ruled out.

281 Firstly, the retention properties of aminopropyl-modified silica and PSA towards sugars has  
282 been ascribed mainly to H-bonding [29]. The role of H-bonding of protonated ethylenediamine based  
283 materials, structurally similar to PSA, in the retention of uncharged compounds is supported by many  
284 authors [30, 31], who also speculated on possible leading retention mechanisms via H-bonding as a  
285 function of pH and on the abundancy of  $NH_3^+/NH_2$  and  $NH_3^+/NH$  groups [31].

286 As shown in Fig. 3, for all the adsorbents, retention capabilities decrease at increasing pH.  
287 This may be ascribed to a change of the relative population of protonated and deprotonated amine  
288 groups and to their involvement in H-bonding. At increasing pH, the population of protonated amines  
289 decreases. Since protonated amines are stronger Brønsted acids than amines, they may be considered  
290 also stronger H donor in H-bonding.

291 Data in Fig. 3A-3B-3C show that SBA-15-AN has higher retention abilities than SBA-15-  
292 APTES at all the pH values tested ( $SBA-15-AN > SBA-15-APTES > PSA$ ). Indeed, if we consider  
293 that aniline ( $pK_b$  8.9) is a weaker base than propylamine ( $pK_b$  3.5), the decrease of protonated amine  
294 population upon increasing pH is expected to be relatively larger in SBA-15-AN than SBA-15-  
295 APTES. Thus, it may be proposed that H-bonding between protonated amines and sugar molecules,

296 where the former act as proton donor and the latter as proton acceptor, does not play the only role in  
297 the adsorption.

298 Therefore, the better performance of SBA-15-AN compared to that of SBA-15-APTES can  
299 be ascribed to a higher hydrophobicity of the material due to the more hydrophobic functional group,  
300 which is usually desired in case of organic molecules adsorption from water solution. Moreover, the  
301 electron-withdrawing effect of the aromatic ring enhances the positive charge of the ammonium  
302 group, increasing the strength of H-bonding with sugar molecules.

303 Experimental tests indicated that pH 2.1 is the optimal pH value to achieve the highest sugars  
304 adsorption in a QuEChERS application.

305

### 306 *3.3 Organically modified mesoporous silicas in the d-SPE cleanup of QuEChERS*

307 In a QuEChERS procedure, after extraction with acetonitrile, a clean-up step performed in *d*-  
308 SPE is necessary to remove coextracted interferents without losing analytes of interest.

309 To this purpose, the capabilities of SBA-15-APTES and SBA-15-AN as *d*-SPE sorbents were  
310 investigated in the determination of persistent pollutants (PAHs and PCBs, included dioxine-like  
311 congeners) in strawberries, using the QuEChERS extraction approach.

312 Performances of the modified silicas were studied and compared with those of PSA,  
313 measuring both signal-to-noise ratio (S/N) and extraction recovery (ER) of PAHs and PCBs after the  
314 application of the QuEChERS protocol.

315 S/N is a parameter characteristic of the chromatogram and indicates the quantification  
316 accuracy of the components during the analytical separation. The higher the S/N, the better  
317 recognized the analyte and the lower the detection limits obtainable. Due to this intrinsic property,  
318 S/N is considered a primary standard for comparison of chromatographic performances [32] and it is  
319 therefore frequently used as response in analytical design optimizations [32-34]. In a complex matrix,  
320 such as strawberry rich in sugars, anthocyanins and polyphenols [35], S/N is indicative of the  
321 efficiency of matrix removal.

322 Additionally, ER was also measured, since it is indicative of the efficiency of the whole  
323 method (extraction and cleanup) to extract analytes of interest, without losing them by adsorption  
324 during the clean-up step.

325 Results obtained by our study for S/N are reported in Fig. 4 (PAHs) and 5 (PCBs) while ER  
326 values are shown in Fig. 6 (PAHs) and 7 (PCBs). Data obtained in the absence of the *d*-SPE treatment  
327 were also considered.

328 For an easier interpretation, for each sorbent, experimental results for PAHs are shown, in Fig.  
329 4 and 6, as single value or as average for compounds: up to four benzene rings (acenaphtylene, the

330 isomers: phenanthrene/anthracene; fluorene/pyrene; benzo[a]anthracene/chrysene);  
331 four benzene rings around a 5-membered ring and five benzene rings (the isomers:  
332 benzo[b]fluoranthene/benzo[k]fluoranthene/benzo[a]pyrene); five benzene rings or five benzene  
333 rings around a 5-membered ring (dibenzo[a,h]anthracene and the isomers indeno[1,2,3-  
334 cd]pyrene/benzo[ghi]perylene). For PCBs, for each sorbent, experimental results were shown, in Fig.  
335 5 and 7, as single value or as average for the 14 congeners tested.

336 As regards S/N values, for all the analytes (Fig. 4 and 5), the values obtained without a *d*-SPE  
337 treatment are the lowest, indicating a poor quality of the analytical method. The increase of S/N values  
338 in the presence of the *d*-SPE treatment indicates a better detectability, essentially due to the removal  
339 of coextracted matrix compounds, and the consequent improvement of the baseline. In this regard,  
340 both the organically modified mesoporous silica are effective in improving the analytical method.

341 For PAHs (Fig. 4), S/N obtained with PSA are higher than those obtained with SBA-15-  
342 APTES and SBA-15-AN for all the hydrocarbons, except for the last three heaviest compounds for  
343 which SBA-15-AN is the best performing *d*-SPE sorbent. The improvement of S/N for these last  
344 compounds (about 30%) turns to be important in the enhancement of the detection limits in real  
345 matrices, since the heaviest compounds are affected by poor detectability.

346 For PCBs (Fig. 5), the highest S/N is observed for SBA-15-AN, for which, on average, an  
347 improvement of S/N values of about 20% in respect to PSA is observed.

348 Extraction recovery ER% as a function of the *d*-SPE sorbent used is shown in Fig. 6 for PAHs  
349 and in Fig. 7 for PCBs.

350 For the 13 PAHs, average ER% follows the order PSA (76±19 %) > SBA-15-AN (63±7 %) >  
351 SBA-15-APTES (61±14 %), even though comparable performances are observed for PSA and SBA-  
352 15-AN for lower molecular weight PAHs. Differently, ER% obtained without any *d*-SPE sorbent are  
353 significantly lower, ranging from 14±3 to 25±2% (data not shown).

354 According to the Anova test ( $p=0.0001$ , 95% confidence interval), the average ER for PSA is  
355 statistically different from SBA-15-AN and SBA-15-APTES, whereas average ER for the two  
356 organically modified mesoporous silica do not show statistical difference. Despite the higher ER  
357 obtained for PSA, the lower standard deviation observed for SBA-15-AN indicates that the *d*-SPE  
358 cleanup with SBA-15-AN is more reliable than the one performed with PSA. Statistic variability of  
359 ER% values for each sorbent was also evaluated through Horwitz equation (Thompson modification  
360 [36]), calculating at first the concentration of each PAH, according to its extraction yields, and finally  
361 the maximum acceptable RSD%. Since the maximum acceptable RSD% value calculated was 22%,  
362 the average RSD% values observed for PAHs with each sorbent (26.2% for PSA and 14.2% for SBA-  
363 15-AN) indicate that the use of PSA provided recoveries falling outside the range of acceptability.

364 Differently, the reliability of SBA-15-AN is confirmed since average RSD% is far below the Horwitz  
365 value.

366 Data shows that for all the *d*-SPE sorbents, a decrease of ER% is observed with the increase  
367 of molecular weight introduced by the aromatic rings. This behaviour was verified for PSA also by  
368 Sadowska-Rociak et al [37] in the analysis of PAHs in tea.

369 Even if, overall, PSA is the best performing sorbent for all PAHs, SBA-15-APTES provides  
370 higher ER% for higher molecular weight PAHs.

371 For PCBs, average ER% follows the order PSA ( $92\pm 6\%$ ) > SBA-15-AN ( $88\pm 9\%$ ) > SBA-  
372 15-APTES ( $67\pm 17\%$ ). Again, poor recovery is observed without any *d*-SPE step (ER% ranging from  
373  $36\pm 6$  to  $44\pm 7\%$ , data not shown). The average ER values obtained for PSA and SBA-15-AN are not  
374 statistically different (Anova test,  $p=0.0001$ , 95% confidence interval), whereas average ER values  
375 obtained with SBA-15-APTES statistically differ from those obtained by PSA and SBA-15-AN.  
376 Again, the application of the Horwitz equation (calculated  $RSD\%=22\%$ ), confirmed the statistical  
377 acceptability for recoveries obtained with PSA and SBA-15-AN ( $RSD\%=7.2\%$  and  $10.2\%$ ,  
378 respectively), but not with SBA-15-APTES ( $RSD\%=25.8\%$ ).

379 Presuming that the extraction recovery calculation used compensates for any matrix effect, it  
380 is reasonable to assume that differences in extraction recovery values observed among the three *d*-  
381 SPE materials is due to the different extent of adsorption of PAHs and PCBs by each sorbent, being  
382 the extraction procedure the same for the three tests.

383 For each sorbent, PCBs exhibit higher ER% values than PAHs. For each *d*-SPE sorbent, for  
384 PAHs an increase of ER% is observed upon decreasing molecular weight (MW), showing a partial  
385 anticorrelation (the higher the MW, the lower the ER%) for SBA-15-AN ( $ER\% = -1.9 MW + 346$ ,  
386  $r^2= 0.919$ ) and for SBA-15-APTES ( $ER\% = -3.3 MW + 424$ ,  $r^2= 0.840$ ), while for PSA this behaviour  
387 is not well evidenced ( $ER\% = -1.5 MW + 340$ ,  $r^2= 0.429$ ). This suggests that at variance with what  
388 hypothesized by Dachs and Bayona [38] for silica based octadecyl substrates, in this case, steric  
389 hindrance and shape selectivity do not play a crucial role in the extraction. To explain the higher  
390 extent of adsorption observed for higher molecular weight PAHs, density functional theory (DFT)  
391 simulations were calculated by the software Gaussview 6.0 in order to estimate the potential and  
392 charge density distribution for each PAH tested [39].

393 Results obtained (Fig.8) show that the centre of each ring on both sides of the PAH molecular  
394 plane is negatively charged and corresponds with delocalized  $\pi$  electrons. Indeed, the area of the  $\pi$ -  
395 electron plane spatially increases when the number of rings increased, as demonstrated also by Yang  
396 and co-workers [40]. Hence, the heavier molecular weight of the PAHs offers higher surface  
397 availability for interaction with positively charged amino groups. Moreover, such behaviour is also

398 in agreement with stronger Van der Waals interactions. Conversely, for PCBs, the addition of chlorine  
399 atoms on the biphenyl structure enhances steric hindrance, in agreement with observations of Dachs  
400 and Bayona [38]. In Fig. 9, as an example, the different behaviour of PAHs (Fig. 9A) and PCBs (Fig.  
401 9B) is compared for SBA-15-AN.

402 Eventually the polarity of micropollutants was also considered. Variations in logP does not  
403 significantly influence the extraction performance of the QuEChERS method when SBA-15-APTES  
404 or SBA-15-AN are used as d-SPE sorbents. Instead, an apparent correlation of ER% with log P for  
405 both PAHs and PCBs classes is observed only for PSA ( $ER\% = 10.36 \log P + 0.49$ ,  $r^2=0.653$ ),  
406 highlighting possible limitations in its use of this d-SPE sorbent for more polar analytes. This  
407 observation agrees with what found by Scordo et al. [1] in the extraction of perfluoroalkyl acids from  
408 strawberry.

409

#### 410 **4. Conclusions**

411 SBA-15 mesoporous silica were functionalized with (3-aminopropyl)-triethoxysilane (SBA-  
412 15-APTES) and N-[3-(Trimethoxysilyl)propyl]aniline (SBA-15-AN) and used for the first time as d-  
413 SPE sorbents in the removal of coextracted compounds (e.g. sugars) in the QuEChERS protocol  
414 applied for the determination of micropollutants (PAHs and PCBs) in strawberry. SBA-15-APTES  
415 and SBA-15-AN were physico-chemically characterized and compared with PSA, the d-SPE sorbent  
416 usually employed in QuEChERS application. The removal capabilities of SBA-15-APTES and SBA-  
417 15-AN towards glucose, sucrose and fructose, chosen as model sugars present in strawberry was  
418 observed to be higher than that of PSA, due to the higher amount of adsorption active sites. A  
419 thorough study of the effect of pH on removal of sugars allowed to propose an interaction mechanism  
420 between amines and sugar molecules mainly based on H-bonding.

421 The suitability of SBA-15-APTES and SBA-15-AN as d-SPE sorbents were confirmed  
422 including these sorbents in the clean-up step of a QuEChERS protocol for the determination of PAHs  
423 and PCBs in intentionally contaminated strawberries. Signal-to-noise ratio for PCBs can be  
424 significantly reduced by SBA-15-AN, indicating even a more efficient cleanup if compared to PSA.  
425 It is worth remembering that the reduction of signal-to-noise ratio is important to determine lower  
426 concentrations of micropollutants in food. Overall, QuEChERS protocol performed by SBA-15-AN  
427 provides slightly lower or comparable extraction recoveries than PSA ( $63\pm 7\%$  vs  $76\pm 19\%$  for PAHs,  
428 respectively and  $92\pm 6\%$  vs  $88\pm 9\%$  for PCBs) and better reproducibility of the method. Molecular  
429 weight of the target micropollutants, but not log P, seem to influence the overall QuEChERS  
430 extraction recovery in the organically modified SBA-15.

431

432 **Declaration of Competing Interest**

433 The authors declare that they have no known competing financial interests or personal  
434 relationships that could have appeared to influence the work reported in this paper.

435

436 **Supplementary Information**

437 The manuscript contains supplementary material.

438

439 **CRedit author statement**

440 **M. Castiglioni:** investigation, writing original draft, manuscript revision. **B. Onida:** data  
441 interpretation, review and manuscript editing. **L. Rivoira:** supervision, data validation and curation,  
442 manuscript revision. **M. Del Bubba:** data interpretation, manuscript editing. **S. Ronchetti:** data  
443 interpretation, review. **M.C. Bruzzoniti:** conceptualization, data interpretation, review and  
444 manuscript editing, funding acquisition, manuscript revision.

445

446 **Acknowledgements**

447 Financial supports from Ministero della Ricerca e dell'Università (MUR, Italy), PRIN 2017  
448 (017PMR932) and Ex-60% are gratefully acknowledged.

449

450

451 **References**

- 452 [1] C.V.A. Scordo, L. Checchini, L. Renai, S. Orlandini, M.C. Bruzzoniti, D. Fibbi, L. Mandi, N. Ouazzani, M. Del  
453 Bubba, Optimization and validation of a method based on QuEChERS extraction and liquid  
454 chromatographic–tandem mass spectrometric analysis for the determination of perfluoroalkyl acids in  
455 strawberry and olive fruits, as model crops with different matrix characteristics, *J. Chromatogr. A* 1621  
456 (2020) 461038. <https://doi.org/https://doi.org/10.1016/j.chroma.2020.461038>.
- 457 [2] L. Rivoira, M. Castiglioni, A. Kettab, N. Ouazzani, E. Al-Karablieh, N. Boujelben, D. Fibbi, E. Coppini, E.  
458 Giordani, M.D. Bubba, M.C. Bruzzoniti, Impact of effluents from wastewater treatments reused for  
459 irrigation: Strawberry as case study, *Environmental Engineering and Management Journal* 18(10) (2019)  
460 2133-2143.
- 461 [3] K. Grob, M. Biedermann, E. Scherbaum, M. Roth, K. Rieger, Food contamination with organic materials  
462 in perspective: packaging materials as the largest and least controlled source? A view focusing on the  
463 European situation, *Critical reviews in food science and nutrition* 46(7) (2006) 529-535.  
464 <https://doi.org/10.1080/10408390500295490>.
- 465 [4] L. Sung-Jin, O. Young-Tak, J. You-Sung, R. Jin-Ho, C. Geun-Hyoung, Y. Ji-Yeon, P. Byung-Jun, Persistent  
466 organic pollutants (POPs) residues in greenhouse soil and strawberry organochlorine pesticides, *Korean*  
467 *Journal of Environmental Agriculture* 35(1) (2016) 6-14.  
468 <https://doi.org/https://doi.org/10.5338/KJEA.2016.35.1.05>.
- 469 [5] European Commission, 2014/663/EU: Commission Recommendation of 11 September 2014 amending  
470 the Annex to Recommendation 2013/711/EU on the reduction of the presence of dioxins, furans and PCBs  
471 in feed and food Text with EEA relevance, (2014).

472 [6] M. Anastassiades, S.J. Lehotay, D. Stajnbaher, F.J. Schenck, Fast and easy multiresidue method  
473 employing acetonitrile extraction/partitioning and "dispersive solid-phase extraction" for the determination  
474 of pesticide residues in produce, *J. AOAC Int.* 86(2) (2003) 412-31.  
475 <https://doi.org/https://doi.org/10.1093/jaoac/86.2.412>.

476 [7] D. Rossini, L. Ciofi, C. Ancillotti, L. Checchini, M.C. Bruzzoniti, L. Rivoira, D. Fibbi, S. Orlandini, M. Del  
477 Bubba, Innovative combination of QuEChERS extraction with on-line solid-phase extract purification and  
478 pre-concentration, followed by liquid chromatography-tandem mass spectrometry for the determination of  
479 non-steroidal anti-inflammatory drugs and their metabolites in sewage sludge, *Anal. Chim. Acta* 935 (2016)  
480 269-281. <https://doi.org/10.1016/j.aca.2016.06.023>.

481 [8] M.C. Bruzzoniti, L. Checchini, R.M. De Carlo, S. Orlandini, L. Rivoira, M. Del Bubba, QuEChERS sample  
482 preparation for the determination of pesticides and other organic residues in environmental matrices: a  
483 critical review, *Anal Bioanal Chem* 406(17) (2014) 4089-4116. <https://doi.org/10.1007/s00216-014-7798-4>.

484 [9] D. Oshita, I.C.S.F. Jardim, Comparison of Different Sorbents in the QuEChERS Method for the  
485 Determination of Pesticide Residues in Strawberries by LC-MS/MS, *Chromatographia* 77(19) (2014) 1291-  
486 1298. <https://doi.org/10.1007/s10337-014-2726-5>.

487 [10] Y. He, Y.-H. Liu, Assessment of primary and secondary amine adsorbents and elution solvents with or  
488 without graphitized carbon for the SPE clean-up of food extracts in pesticide residue analysis,  
489 *Chromatographia* 65(9-10) (2007) 581-590. <https://doi.org/https://doi.org/10.1365/s10337-007-0198-6>.

490 [11] Z. Wu, D. Zhao, Ordered mesoporous materials as adsorbents, *Chem. Commun.* 47(12) (2011) 3332-  
491 3338. <https://doi.org/10.1039/C0CC04909C>.

492 [12] C.M. Li, X.P. Wang, Z.H. Jiao, Y.S. Zhang, X.B. Yin, X.M. Cui, Y.Z. Wei, Functionalized Porous Silica-Based  
493 Nano/Micro Particles for Environmental Remediation of Hazard Ions, *Nanomaterials* 9(2) (2019) 247.  
494 <https://doi.org/https://doi.org/10.3390/nano9020247>.

495 [13] P. Kumar, V.V. Gulians, Periodic mesoporous organic-inorganic hybrid materials: applications in  
496 membrane separations and adsorption, *Microporous Mesoporous Mater.* 132(1-2) (2010) 1-14.  
497 <https://doi.org/https://doi.org/10.1016/j.micromeso.2010.02.007>.

498 [14] M.C. Bruzzoniti, E. Mentasti, C. Sarzanini, B. Onida, B. Bonelli, E. Garrone, Retention properties of  
499 mesoporous silica-based materials, *Anal. Chim. Acta* 422(2) (2000) 231-238.  
500 [https://doi.org/10.1016/S0003-2670\(00\)01070-9](https://doi.org/10.1016/S0003-2670(00)01070-9).

501 [15] N. Casado, D. Pérez-Quintanilla, S. Morante-Zarcelero, I. Sierra, Current development and applications of  
502 ordered mesoporous silicas and other sol-gel silica-based materials in food sample preparation for  
503 xenobiotics analysis, *TrAC, Trends Anal. Chem.* 88 (2017) 167-184.  
504 <https://doi.org/https://doi.org/10.1016/j.trac.2017.01.001>.

505 [16] S. Fiorilli, L. Rivoira, G. Cali, M. Appendini, M.C. Bruzzoniti, M. Coisson, B. Onida, Iron oxide inside SBA-  
506 15 modified with amino groups as reusable adsorbent for highly efficient removal of glyphosate from  
507 water, *Appl. Surf. Sci.* 411 (2017) 457-465. <https://doi.org/10.1016/j.apsusc.2017.03.206>.

508 [17] L. Rivoira, M. Appendini, S. Fiorilli, B. Onida, M. Del Bubba, M.C. Bruzzoniti, Functionalized iron  
509 oxide/SBA-15 sorbent: investigation of adsorption performance towards glyphosate herbicide,  
510 *Environmental Science and Pollution Research* 23(21) (2016) 21682-21691.  
511 <https://doi.org/10.1007/s11356-016-7384-8>.

512 [18] A. Paris, J. Ledauphin, P. Poinot, J.-L. Gaillard, Polycyclic aromatic hydrocarbons in fruits and  
513 vegetables: Origin, analysis, and occurrence, *Environ. Pollut.* 234 (2018) 96-106.  
514 <https://doi.org/https://doi.org/10.1016/j.envpol.2017.11.028>.

515 [19] A.A. Lovett, C.D. Foxall, C.S. Creaser, D. Chew, PCB and PCDD/DF congeners in locally grown fruit and  
516 vegetable samples in Wales and England, *Chemosphere* 34(5) (1997) 1421-1436.  
517 [https://doi.org/https://doi.org/10.1016/S0045-6535\(97\)00439-6](https://doi.org/https://doi.org/10.1016/S0045-6535(97)00439-6).

518 [20] M.C. Bruzzoniti, L. Rivoira, M. Castiglioni, A. El Ghadraoui, A. Ahmali, T. El Hakim El Mansour, L. Mandi,  
519 N. Ouazzani, M. Del Bubba, Extraction of polycyclic aromatic hydrocarbons and polychlorinated biphenyls  
520 from urban and olive mill wastewaters intended for reuse in agricultural irrigation, *J. AOAC Int.* 103(2)  
521 (2020) 382-391. <https://doi.org/10.5740/jaoacint.19-0257>.



522 [21] M.J. Kasperbauer, J.H. Loughrin, S.Y. Wang, Light Reflected from Red Mulch to Ripening Strawberries  
523 Affects Aroma, Sugar and Organic Acid Concentrations, *Photochem. Photobiol.* 74(1) (2001) 103-107.  
524 [https://doi.org/https://doi.org/10.1562/0031-8655\(2001\)0740103LRFRMT2.0.CO2](https://doi.org/https://doi.org/10.1562/0031-8655(2001)0740103LRFRMT2.0.CO2).

525 [22] C.H. Vane, A.W. Kim, D.J. Beriro, M.R. Cave, K. Knights, V. Moss-Hayes, P.C. Nathanail, Polycyclic  
526 aromatic hydrocarbons (PAH) and polychlorinated biphenyls (PCB) in urban soils of Greater London, UK,  
527 *Appl. Geochem.* 51 (2014) 303-314. <https://doi.org/https://doi.org/10.1016/j.apgeochem.2014.09.013>.

528 [23] R.M. De Carlo, L. Rivoira, L. Ciofi, C. Ancillotti, L. Checchini, M. Del Bubba, M.C. Bruzzoniti, Evaluation of  
529 different QuEChERS procedures for the recovery of selected drugs and herbicides from soil using LC  
530 coupled with UV and pulsed amperometry for their detection, *Analytical and Bioanalytical Chemistry* 407(4)  
531 (2015) 1217-1229. <https://doi.org/https://doi.org/10.1007/s00216-014-8339-x>.

532 [24] United States of Pharmacopoeia 38 NF 33, United States Pharmacopeial Convention, General chapter  
533 <621>, Chromatography, 2015, pp. 424-434.

534 [25] D. Brunel, A.C. Blanc, E. Garrone, B. Onida, M. Rocchia, J.B. Nagy, D.J. Macquarrie, Spectroscopic  
535 studies on aminopropyl-containing micelle templated silicas. Comparison of grafted and co-condensation  
536 routes, in: R. Aiello, G. Giordano, F. Testa (Eds.), *Stud. Surf. Sci. Catal.*, Elsevier 2002, pp. 1395-1402.  
537 [https://doi.org/https://doi.org/10.1016/S0167-2991\(02\)80305-6](https://doi.org/https://doi.org/10.1016/S0167-2991(02)80305-6).

538 [26] B. Onida, L. Borello, C. Busco, P. Ugliengo, Y. Goto, S. Inagaki, E. Garrone, The surface of ordered  
539 mesoporous benzene - Silica hybrid material: An infrared and ab initio molecular modeling study, *J. Phys.*  
540 *Chem. B* 109(24) (2005) 11961-11966. <https://doi.org/10.1021/jp050686n>.

541 [27] Y.Y. Ye M., Trinh A., Analysis of Multi-Pesticide Residues in Vegetables, Food, and Fruits by SPE/GC-MS,  
542 available at [https://www.sigmaaldrich.com/content/dam/sigma-](https://www.sigmaaldrich.com/content/dam/sigma-aldrich/docs/Supelco/Posters/t405020h.pdf)  
543 [aldrich/docs/Supelco/Posters/t405020h.pdf](https://www.sigmaaldrich.com/content/dam/sigma-aldrich/docs/Supelco/Posters/t405020h.pdf) last accessed September 2020.

544 [28] O. Shimelis, Y. Yang, K. Stenerson, T. Kaneko, M. Ye, Evaluation of a solid-phase extraction dual-layer  
545 carbon/primary secondary amine for clean-up of fatty acid matrix components from food extracts in  
546 multiresidue pesticide analysis, *J. Chromatogr. A* 1165(1) (2007) 18-25.  
547 <https://doi.org/https://doi.org/10.1016/j.chroma.2007.07.037>.

548 [29] F. Plössl, M. Giera, F. Bracher, Multiresidue analytical method using dispersive solid-phase extraction  
549 and gas chromatography/ion trap mass spectrometry to determine pharmaceuticals in whole blood, *J.*  
550 *Chromatogr. A* 1135(1) (2006) 19-26. <https://doi.org/https://doi.org/10.1016/j.chroma.2006.09.033>.

551 [30] D. Orso, M. Martins, F. Donato, T. Rizzetti, M. Kemmerich, M. Adaime, R. Zanella, Multiresidue  
552 Determination of Pesticide Residues in Honey by Modified QuEChERS Method and Gas Chromatography  
553 with Electron Capture Detection, *Journal of the Brazilian Chemical Society* 25 (2014).  
554 <https://doi.org/10.5935/0103-5053.20140117>.

555 [31] C. Ling, X. Li, Z. Zhang, F. Liu, Y. Deng, X. Zhang, A. Li, L. He, B. Xing, High adsorption of  
556 sulfamethoxazole by an amine-modified polystyrene-divinylbenzene resin and its mechanistic insight,  
557 *Environmental science & technology* 50(18) (2016) 10015-10023.  
558 <https://doi.org/https://doi.org/10.1021/acs.est.6b02846>.

559 [32] G. Wells, H. Prest, C.W. Russ IV, Why use signal-to-noise as a measure of MS performance when it is  
560 often meaningless?, *Technical Overview*, Agilent Technologies (2011) available at  
561 [https://www.google.com/url?sa=t&rct=j&q=&esrc=s&source=web&cd=&cad=rja&uact=8&ved=2ahUKEwiN\\_76uuJPuAhVPCuwKHY\\_cDTUQFjABegQIBxAC&url=https%3A%2F%2Fwww.agilent.com%2Fcs%2Flibrary%2Ftechnicaloverviews%2Fpublic%2F5990-8341EN.pdf&usg=AOvVaw35pJ2yCwYqtgeugpe9ySZj](https://www.google.com/url?sa=t&rct=j&q=&esrc=s&source=web&cd=&cad=rja&uact=8&ved=2ahUKEwiN_76uuJPuAhVPCuwKHY_cDTUQFjABegQIBxAC&url=https%3A%2F%2Fwww.agilent.com%2Fcs%2Flibrary%2Ftechnicaloverviews%2Fpublic%2F5990-8341EN.pdf&usg=AOvVaw35pJ2yCwYqtgeugpe9ySZj).

562  
563  
564 [33] J. Bérubé, C. Wu, Signal-to-noise ratio and related measures in parameter design optimization: an  
565 overview, *Sankhyā: The Indian Journal of Statistics, Series B* (2000) 417-432.

566 [34] L. Rivoira, R.M. De Carlo, S. Cavalli, M.C. Bruzzoniti, Simple SPE-HPLC determination of some common  
567 drugs and herbicides of environmental concern by pulsed amperometry, *Talanta* 131 (2015) 205-212.  
568 <https://doi.org/https://doi.org/10.1016/j.talanta.2014.07.070>.

569 [35] L. Renai, F. Tozzi, C.V. Scordo, E. Giordani, M.C. Bruzzoniti, D. Fibbi, L. Mandi, N. Ouazzani, M. Del  
570 Bubba, Productivity and nutritional and nutraceutical value of strawberry fruits (*Fragaria x ananassa* Duch.)  
571 cultivated under irrigation with treated wastewaters, *J. Sci. Food Agric.* in press (2020).  
572 <https://doi.org/10.1002/jsfa.10737>.

- 573 [36] C. Rivera, R. Rodríguez, Horwitz equation as quality benchmark in ISO/IEC 17025 testing laboratory,  
574 Private communication (2014).
- 575 [37] A. Sadowska-Rociek, M. Surma, E. Cieřlik, Comparison of different modifications on QuEChERS sample  
576 preparation method for PAHs determination in black, green, red and white tea, Environmental Science and  
577 Pollution Research 21(2) (2014) 1326-1338. <https://doi.org/10.1007/s11356-013-2022-1>.
- 578 [38] J. Dachs, J.M. Bayona, Large volume preconcentration of dissolved hydrocarbons and polychlorinated  
579 biphenyls from seawater. Intercomparison between C18 disks and XAD-2 column, Chemosphere 35(8)  
580 (1997) 1669-1679. [https://doi.org/https://doi.org/10.1016/S0045-6535\(97\)00248-8](https://doi.org/https://doi.org/10.1016/S0045-6535(97)00248-8).
- 581 [39] T. Sato, T. Tsuneda, K. Hirao, A density-functional study on  $\pi$ -aromatic interaction: Benzene dimer and  
582 naphthalene dimer, The Journal of chemical physics 123(10) (2005) 104307.  
583 <https://doi.org/https://doi.org/10.1063/1.2011396>.
- 584 [40] X. Yang, C. Zhang, L. Jiang, Z. Li, Y. Liu, H. Wang, Y. Xing, R.T. Yang, Molecular simulation of  
585 naphthalene, phenanthrene, and pyrene adsorption on MCM-41, International journal of molecular  
586 sciences 20(3) (2019) 665. <https://doi.org/https://doi.org/10.3390/ijms20030665>.

587  
588

589 **Figure Captions**

590

591 **Fig. 1.** Schematic representation of PSA (A) and structure of the precursors APTES (B) and  
592 N-[3-(trimethoxysilyl)propyl]aniline (C).

593 **Fig. 2.** FT-IR Spectra of SBA-15 (curve 1), SBA-15-APTES (curve 2) and SBA-15-AN  
594 (curve 3). The spectrum of SBA-15 was amplified by a factor 2 for sake of clarity.

595 **Fig. 3.** Adsorption of glucose, fructose, sucrose on PSA, SBA-15-APTES and SBA-15-AN at  
596 pH 2.1 (A), 5.0 (B) and 8.5 (C). For experimental details, see text.

597 **Fig. 4.** Signal-to-noise ratio (S/N) obtained after the QuEChERS extraction of PAHs from  
598 strawberry, without and with the *d*-SPE clean-up by PSA, SBA-15-APTES and SBA-15-AN. For  
599 QuEChERS extraction conditions, see text.

600 **Fig. 5.** Signal-to-noise ratio (S/N) obtained after the QuEChERS extraction of PCBs from  
601 strawberry, without and with the *d*-SPE clean-up by PSA, SBA-15-APTES and SBA-15-AN. For  
602 QuEChERS extraction conditions, see text.

603 **Fig. 6.** Extraction recovery percentage obtained after the QuEChERS extraction of PAHs  
604 from strawberry and the *d*-SPE clean-up by PSA, SBA-15-APTES and SBA-15-AN. For QuEChERS  
605 extraction conditions, see text.

606 **Fig. 7.** Extraction recovery percentage obtained after the QuEChERS extraction of PCBs  
607 from strawberry and the *d*-SPE clean-up by PSA, SBA-15-APTES and SBA-15-AN. For QuEChERS  
608 extraction conditions, see text.

609 **Fig. 8:** Electrostatic potential and charge density distribution results of target PAHs, listed  
610 following the classes described in paragraph 3.3 (ring classification).

611 At the top of each structure, the colour scale of electrostatic potential distribution (unique for each  
612 PAH) is represented, with the blue (red) portion representing the most positive (negative) potential.

613 **Fig. 9.** Dependence of PAH (A) and PCB (B) extraction recovery percentage on molecular  
614 weight (MW) using SBA-15-AN as *d*-SPE sorbent within the QuEChERS protocol in strawberry.

615

616

617

618

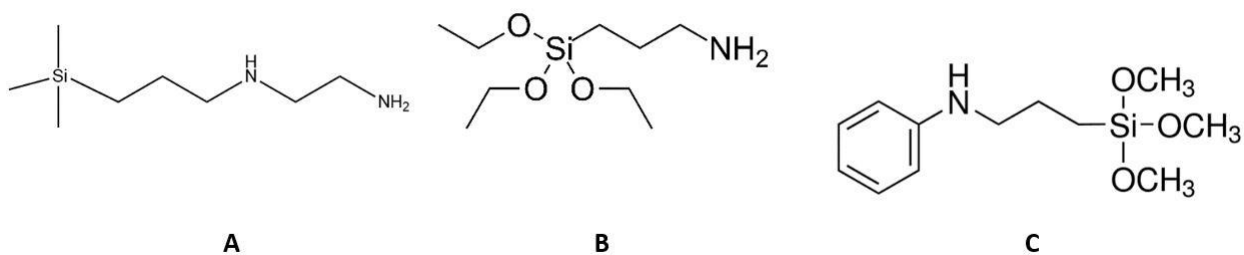


**Fig. 1.** Schematic representation of PSA (A) and structure of the precursors APTES (B) and N-[3-(trimethoxysilyl)propyl]aniline (C).

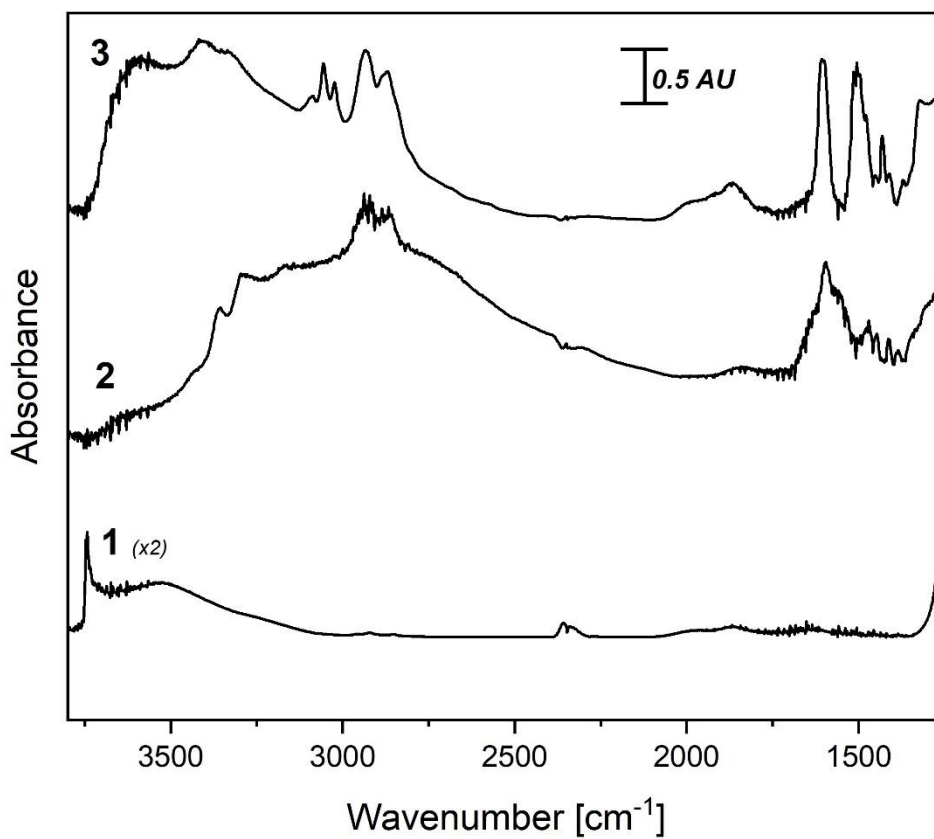
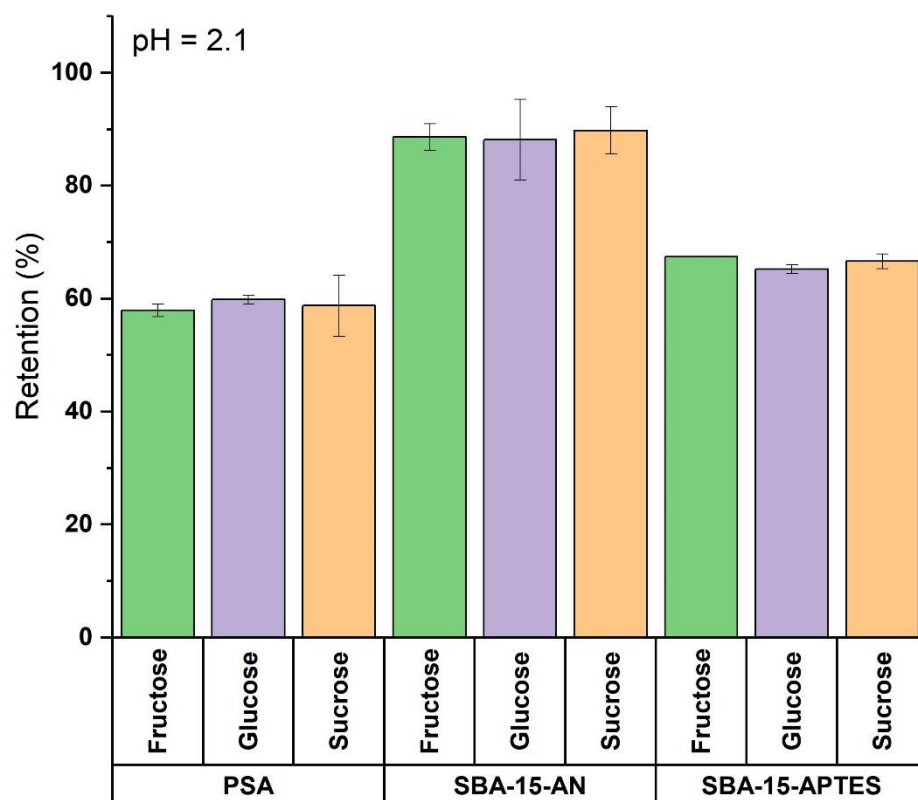
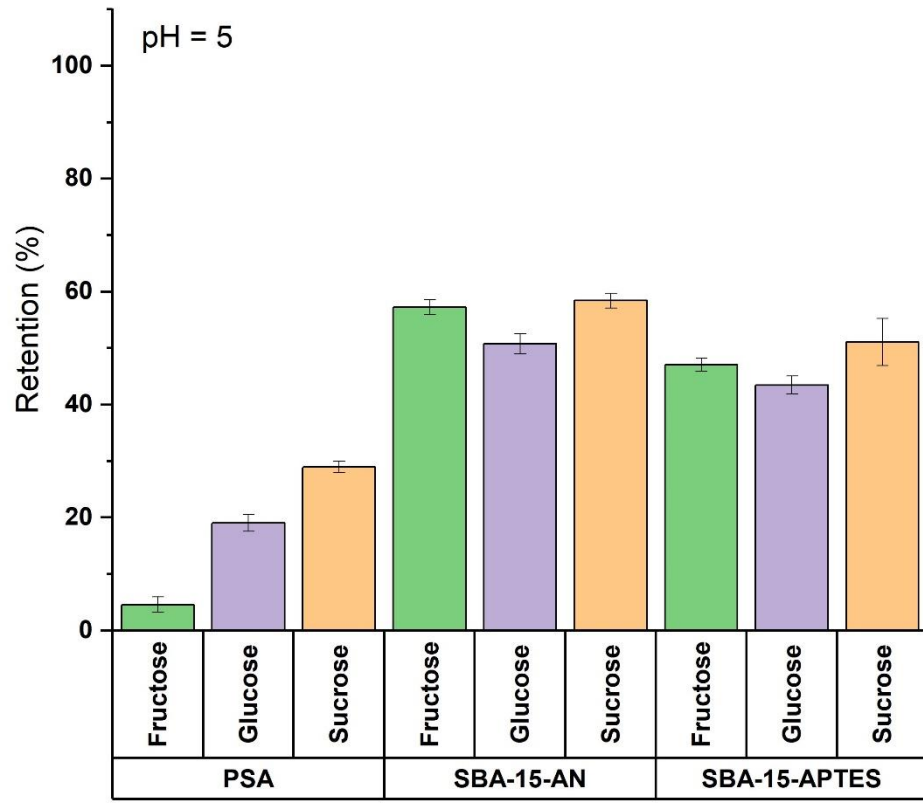


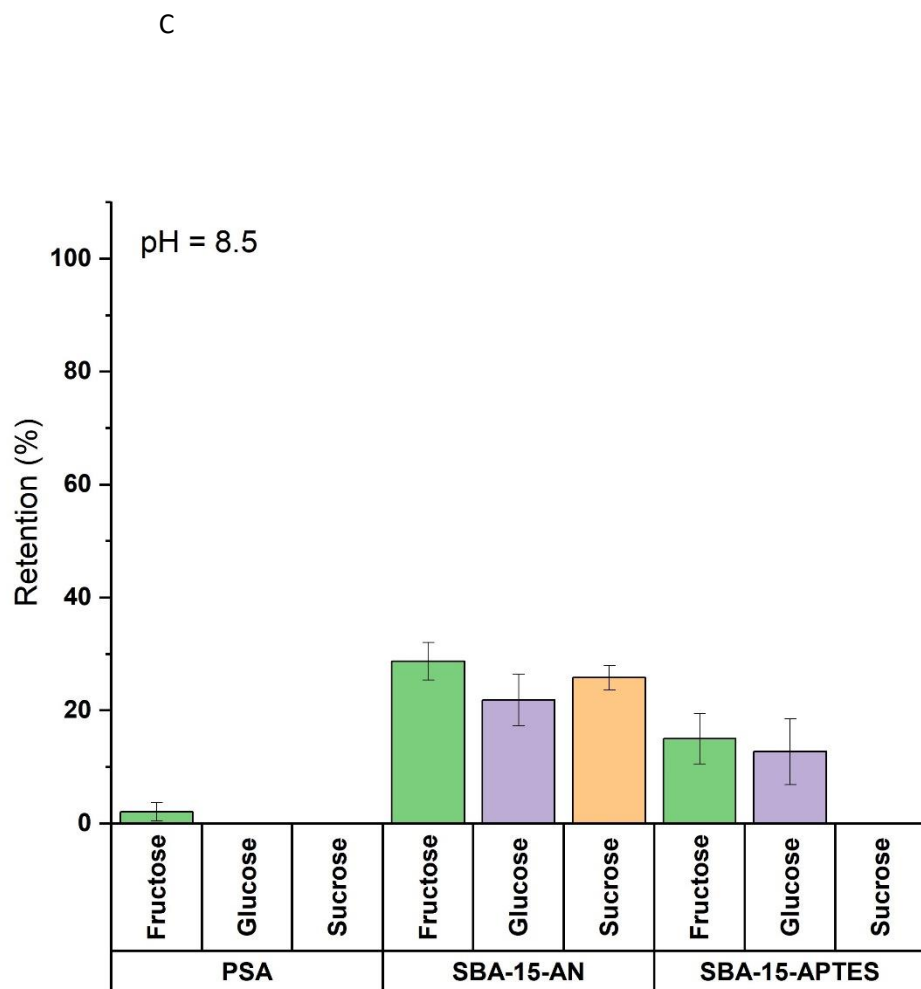
**Fig. 2.** FT-IR Spectra of SBA-15 (curve 1), SBA-15-APTES (curve 2) and SBA-15-AN (curve 3). The spectrum of SBA-15 was amplified by a factor 2 for sake of clarity.

A

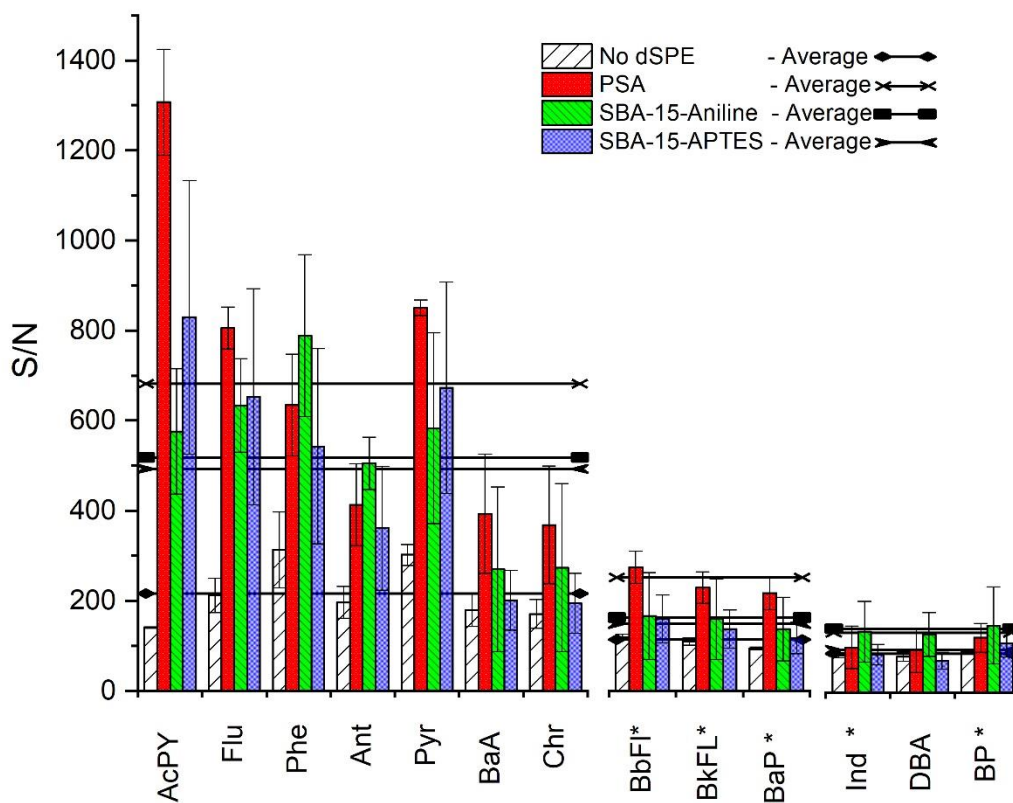


B



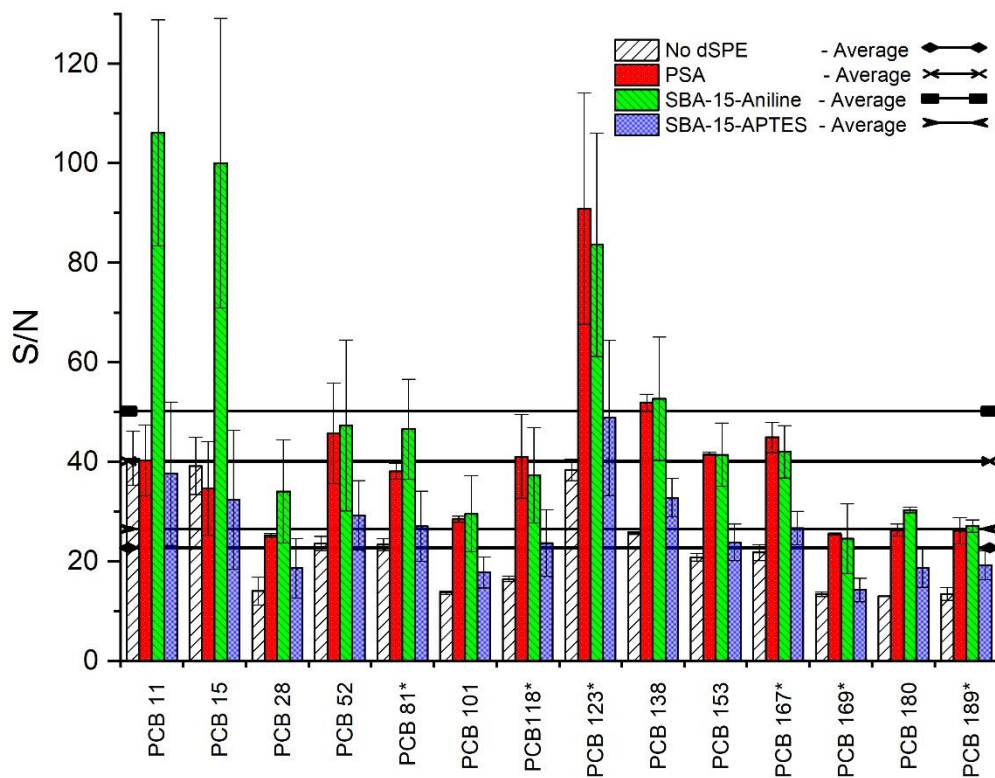


**Fig. 3.** Adsorption of glucose, fructose, sucrose on PSA, SBA-15-APTES and SBA-15-AN at pH 2.1 (A), 5.0 (B) and 8.5 (C). For experimental details, see text.

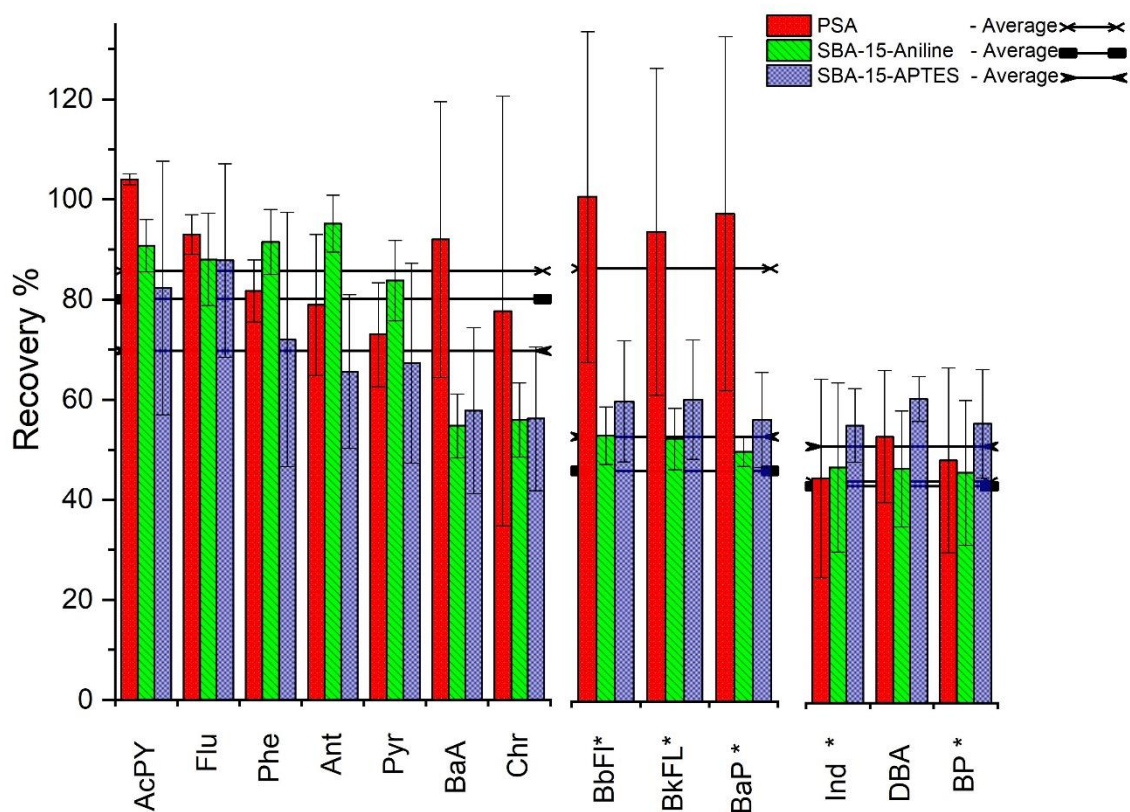


**Fig. 4.** Signal-to-noise ratio (S/N) obtained after the QuEChERS extraction of PAHs from strawberry, without and with the d-SPE clean-up by PSA, SBA-15-APTES and SBA-15-AN. For QuEChERS extraction conditions, see text

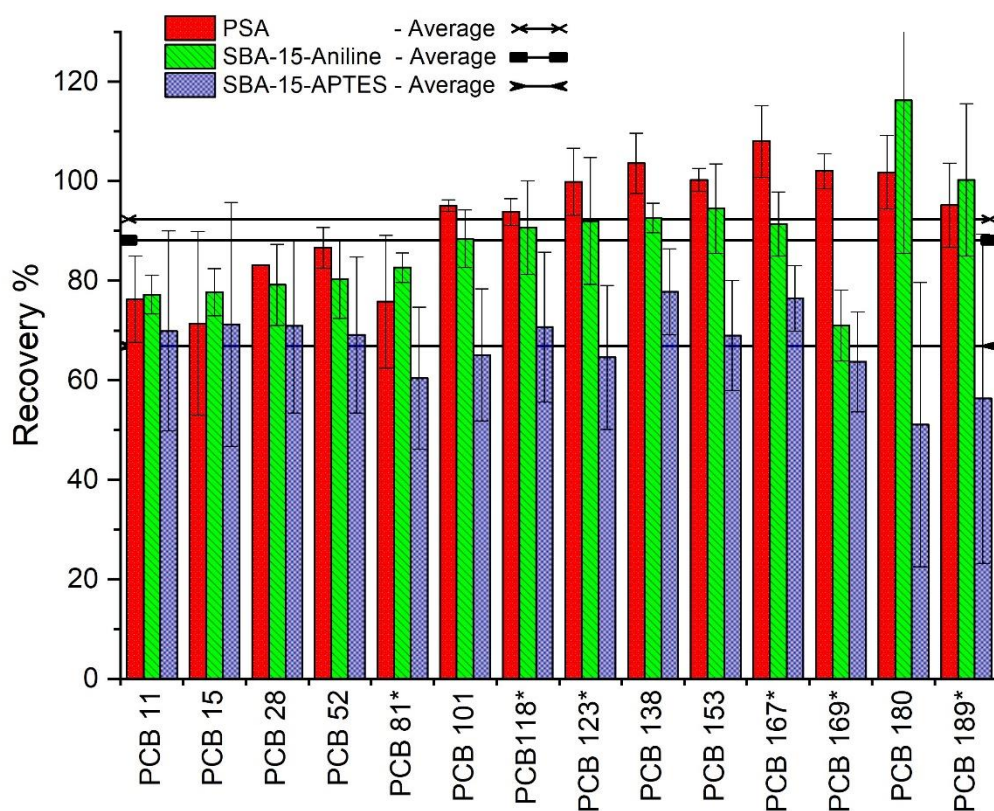




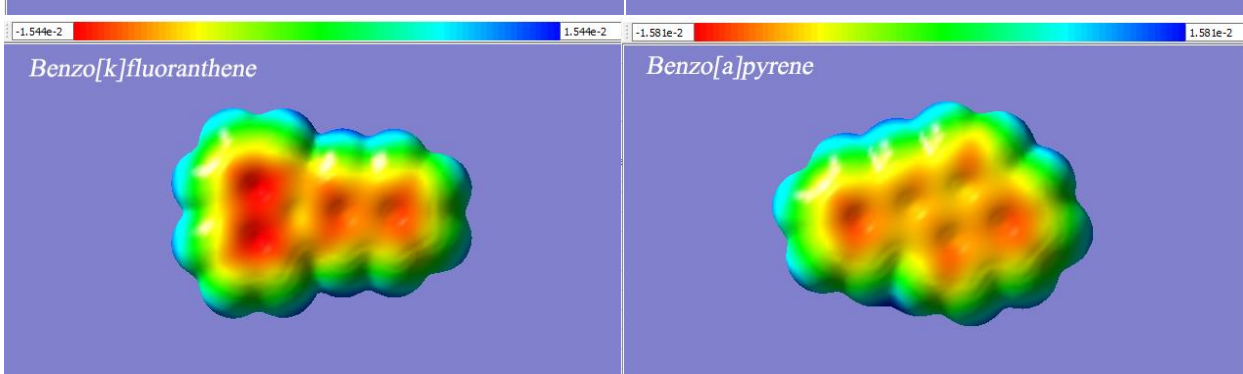
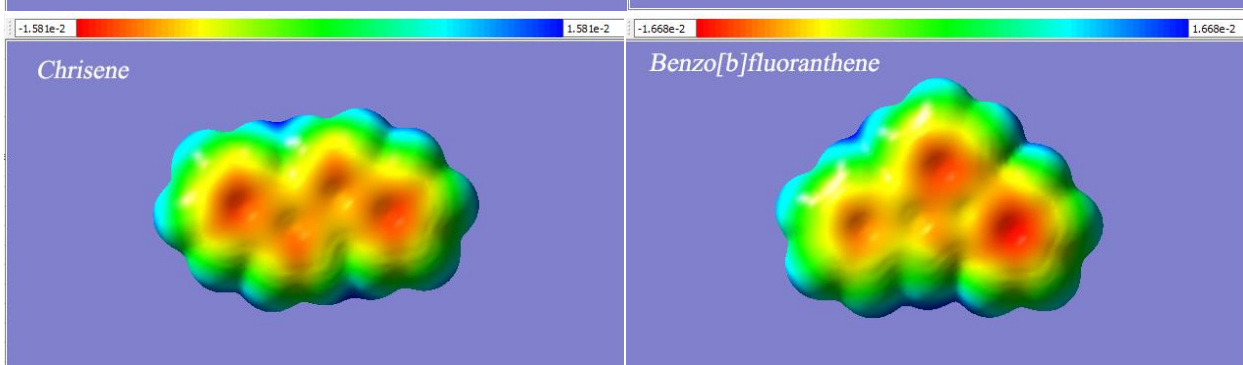
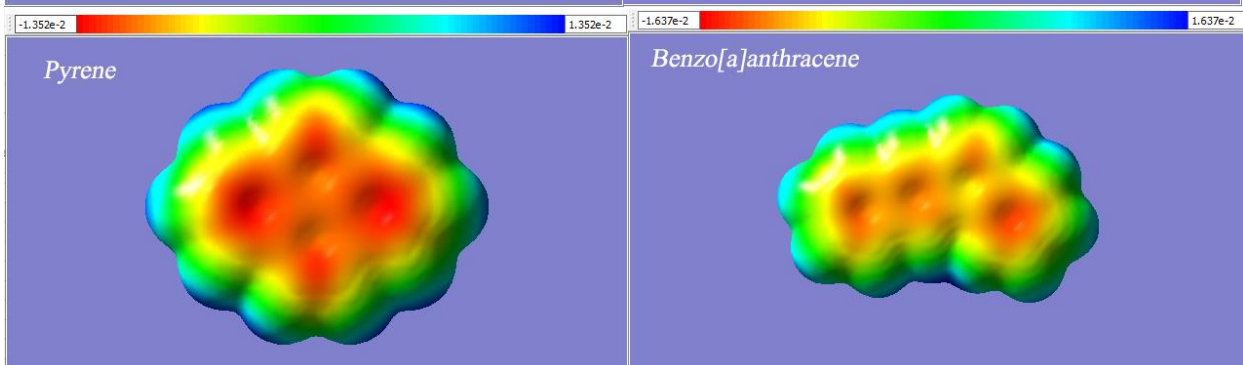
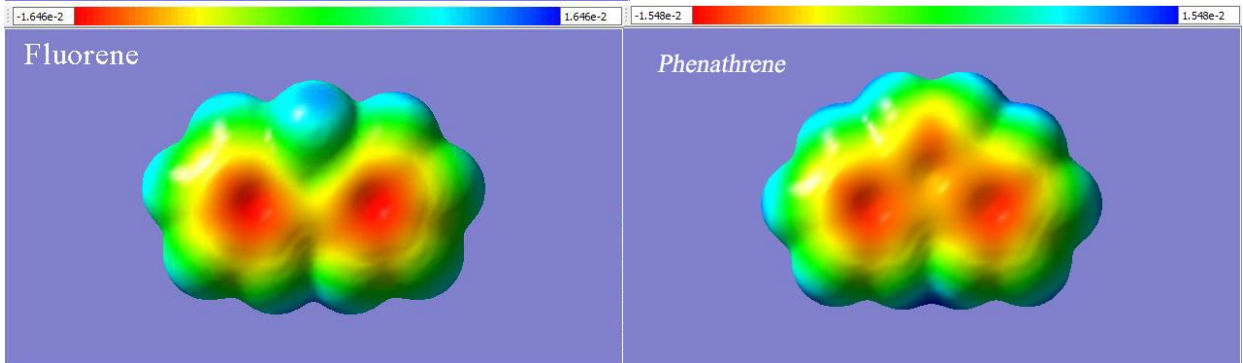
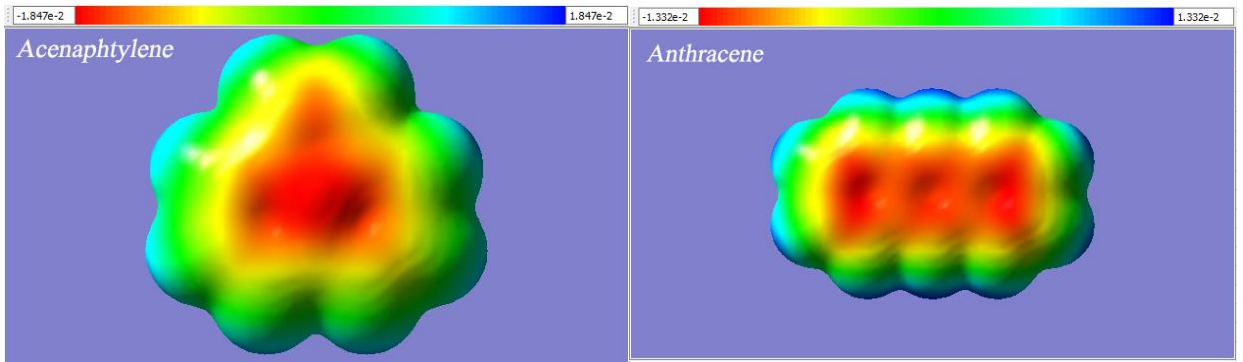
**Fig. 5.** Signal-to-noise ratio (S/N) obtained after the QuEChERS extraction of PCBs from strawberry, without and with the *d*-SPE clean-up by PSA, SBA-15-APTES and SBA-15-AN. For QuEChERS extraction conditions, see text.



**Fig. 6.** Extraction recovery percentage obtained after the QuEChERS extraction of PAHs from strawberry and the *d*-SPE clean-up by PSA, SBA-15-APTES and SBA-15-AN. For QuEChERS extraction conditions, see text.



**Fig. 7.** Extraction recovery percentage obtained after the QuEChERS extraction of PCBs from strawberry and the *d*-SPE clean-up by PSA, SBA-15-APTES and SBA-15-AN. For QuEChERS extraction conditions, see text.



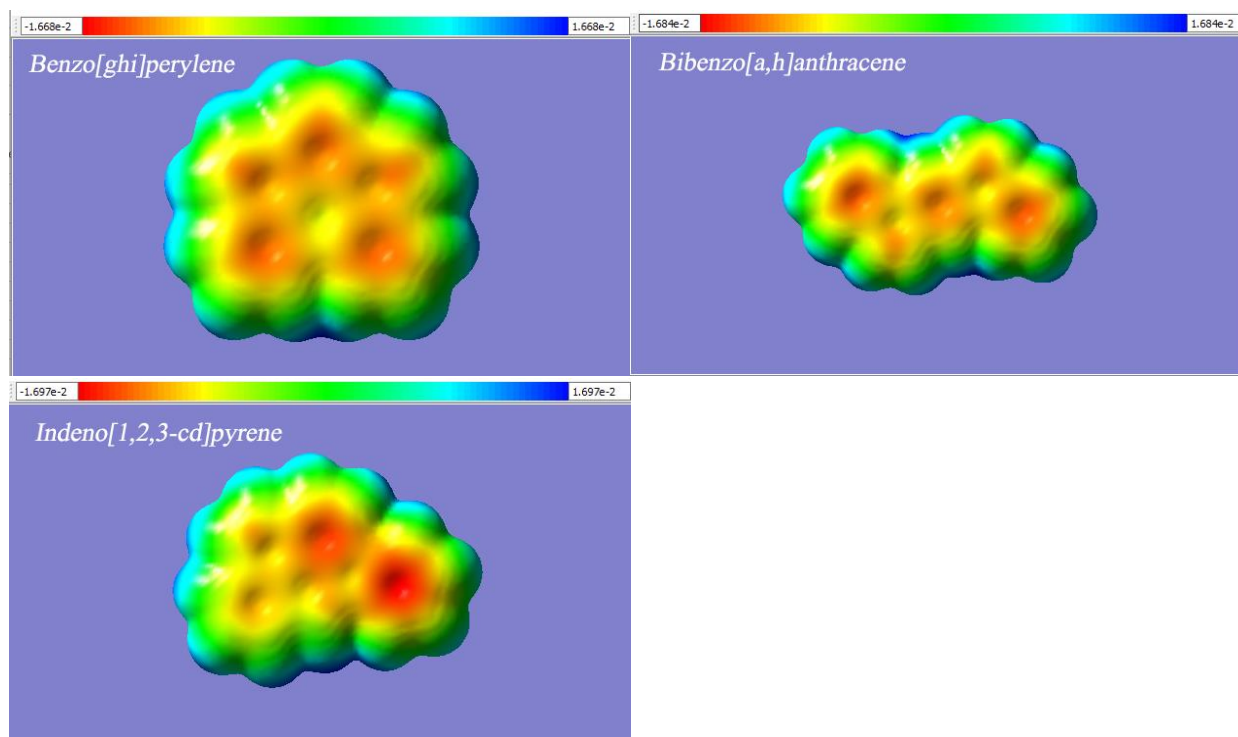
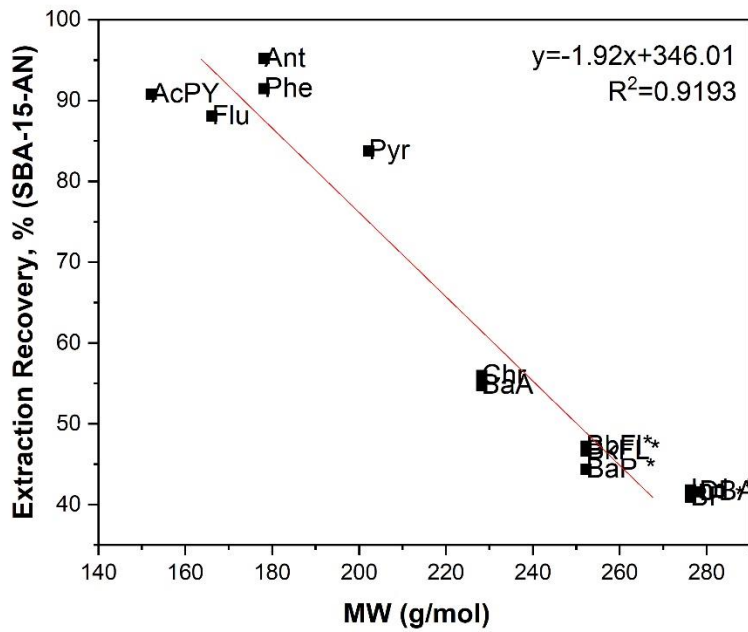


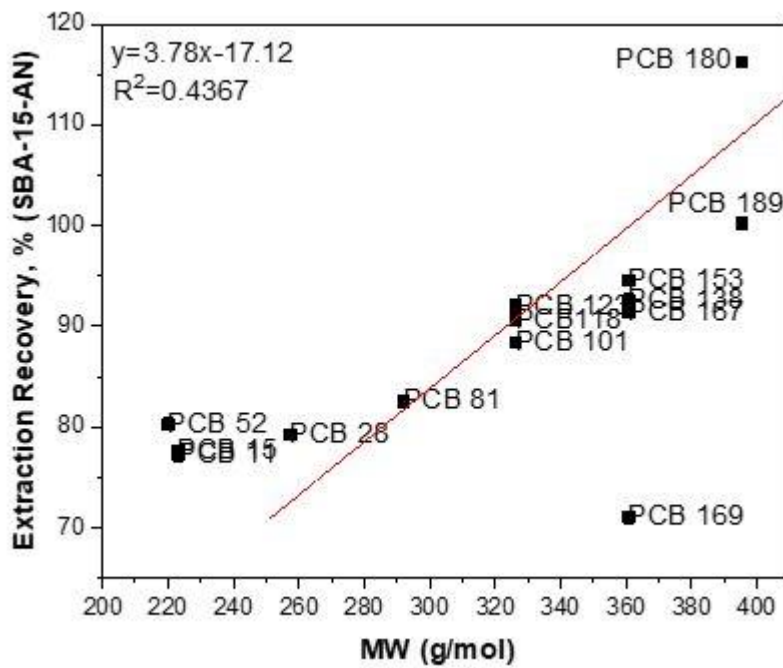
**Fig. 8:** Electrostatic potential and charge density distribution results of target PAHs, listed following the classes described in paragraph 3.3 (ring classification).

At the top of each structure, the colour scale of electrostatic potential distribution (unique for each PAH) is represented, with the blue (red) portion representing the most positive (negative) potential.





A



B

**Fig. 9.** Dependence of PAH (A) and PCB (B) extraction recovery percentage on molecular weight (MW) using SBA-15-AN as *d*-SPE sorbent within the QuEChERS protocol in strawberry.

1 **SUPPLEMENTARY INFORMATION SECTION**

2  
3 **Amino groups modified SBA-15 for dispersive-solid phase extraction in the analysis of**  
4 **micropollutants by QuEChERS approach**

5  
6 Michele Castiglioni<sup>a</sup>, Barbara Onida<sup>b\*</sup>, Luca Rivoira<sup>a</sup>, Massimo Del Bubba<sup>c</sup>, Silvia Ronchetti<sup>b</sup>,  
7 Maria Concetta Bruzzoniti<sup>a\*</sup>

8  
9 <sup>a</sup> Department of Chemistry, University of Turin, Via P. Giuria 7, 10125 Turin, Italy

10 <sup>b</sup> Department of Applied Science and Technology, DISAT, Polytechnic of Turin, Corso Duca degli  
11 Abruzzi 24, 10129 Turin, Italy

12 <sup>c</sup> Department of Chemistry “Ugo Schiff”, University of Florence, Via della Lastruccia 3, 50019  
13 Sesto Fiorentino, Florence, Italy

14  
15 **\*Corresponding Authors**

16 Prof. Maria Concetta Bruzzoniti

17 ORCID ID 0000-0002-9144-9254

18 Department of Chemistry

19 University of Turin

20 Via P. Giuria 7, 10125 Turin, Italy

21  
22 **And**

23  
24 Prof. Barbara Onida

25 ORCID ID 0000-0002-1928-3579

26 Department of Applied Science and Technology

27 DISAT, Polytechnic of Turin

28 Corso Duca degli Abruzzi 24, 10129 Turin, Italy

30 **Table S1.** Main analytical features of the GC-MS method for the determination of PAHs.  
 31 Chromatographic conditions are detailed in paragraph 2.4 of the main manuscript.

PAHs	Slope	Intercept	R <sup>2</sup>	LOD (µg/L)	LOQ (µg/L)
<b>AcPY</b>	1.37	-0.0034	0.9988	0.07	0.22
<b>Flu</b>	1.88	0.0028	0.9984	0.14	0.43
<b>Phe</b>	2.12	0.039	0.9685	0.48	1.46
<b>Ant</b>	0.77	0.003	0.9931	0.15	0.45
<b>Pyr</b>	1.57	0.0076	0.9971	0.13	0.4
<b>BaA</b>	0.91	0.00002	0.9992	0.06	0.18
<b>Chr</b>	1.23	-0.0009	0.9982	0.12	0.35
<b>BbFl</b>	3.7	-0.004	0.9978	0.38	1.15
<b>BkFl</b>	2.76	-0.0041	0.9981	0.27	0.82
<b>BaP</b>	4.12	0.00002	0.9988	0.36	1.07
<b>Ind</b>	5.45	-0.0046	0.9914	1.69	5.12
<b>DBA</b>	4.56	-0.0036	0.9824	2.1	6.36
<b>BP</b>	6.96	-0.0019	0.9976	1.36	4.11

32

33 Linearity range: 0.1- 20 µg/L

34 Intra-day repeatability (n=10): 5.2%

35 Inter-day repeatability (three days, 10 repetitions for each day, n=30): 9.8%

36

37 **Table S2.** Main analytical features of the GC-MS method for the determination of PCBs.

38 Chromatographic conditions are detailed in paragraph 2.4 of the main manuscript.

PCBs	Slope	Intercept	R <sup>2</sup>	LOD (µg/L)	LOQ (µg/L)
<b>PCB 11</b>	4.12	-0.048	0.9982	4.96	14.93
<b>PCB 15</b>	2.62	-0.05	0.9989	2.16	6.55
<b>PCB 28</b>	1.05	-0.026	0.9979	2.99	9.05
<b>PCB 52</b>	1.21	-0.03	0.9982	2.46	7.47
<b>PCB 81</b>	0.87	-0.032	0.9982	1.66	5.04
<b>PCB 101</b>	0.66	-0.014	0.9986	2.03	6.14
<b>PCB 118+123</b>	2.96	-0.064	0.9983	2.87	8.71
<b>PCB 138</b>	1.57	-0.024	0.998	4.31	13.05
<b>PCB 153</b>	0.15	-0.021	0.9981	0.49	1.49
<b>PCB 167</b>	1.23	-0.022	0.9985	2.98	9.04
<b>PCB 169</b>	4.51	-0.046	0.9985	5.4	16.35
<b>PCB 180</b>	0.89	-0.014	0.9981	3.77	11.43
<b>PCB 189</b>	1.07	-0.017	0.9981	4.14	12.54

39

40 Linearity range: 1.5- 25 µg/L

41 Intra-day repeatability (n=10): 4.3%

42 Inter-day repeatability (three days, 10 repetitions for each day, n=30): 9%

43